RESEARCH ARTICLE SUMMARY

HIV

Engineered deletions of HIV replicate conditionally to reduce disease in nonhuman primates

Fathima N. Nagoor Pitchai†, Elizabeth J. Tanner†, Neha Khetan, Gustavo Vasen, Clara Levrel, Arjun J. Kumar, Shilpi Pandey, Tracy Ordonez, Philip Barnette, David Spencer, Seung-Yong Jung, Joshua Glazier, Cassandra Thompson, Alicia Harvey-Vera, Hye-In Son, Steffanie A. Strathdee, Leo Holguin, Ryan Urak, John Burnett, William Burgess, Kathleen Busman-Sahay, Jacob D. Estes, Ann Hessell, Christine M. Fennessey, Brandon F. Keele, Nancy L. Haigwood, Leor S. Weinberger*

INTRODUCTION: Rapidly evolving communicable pathogens, such as HIV, pose stubborn problems for conventional medical countermeasures. Because of substantial viral genetic diversity, there is no approved HIV vaccine. Although combination antiretroviral therapy (ART) is effective, ART is not curative and must be continually administered (discontinuation results in viral rebound), leading to major logistical challenges. Thus, despite decades of intense research, 1 to 2 million new HIV infections occur each year, with the virus overly impacting underprivileged and underserved communities. New antiviral strategies with reduced administration frequencies and high genetic barriers to the evolution of resistance are needed.

RATIONALE: Theories proposed decades ago predicted that HIV viral-deletion variants—based on the historical concept of defective interfering particles (DIPs), which parasitize wild-type viruses—could act as therapeutics. Putative therapeutic interfering particles (TIPs), a subset of DIPs, if rationally engineered to conditionally replicate with a basic reproductive ratio $R_0 > 1$, were predicted to be single-administration, escape-resistant antiviral therapies. Notably, the $R_0 > 1$ conditional replication criterion imparts TIPs with the potential to act as single-dose "drive" therapeutics, thereby overcoming extant therapy barriers. In this work, we developed a TIP for HIV.

RESULTS: Theory-driven in vitro studies showed that long-term HIV-infected bioreactors exhibited von Magnus—like oscillations (a signature of DIPs) and revealed a variant with a ~2.5-kb deletion in the HIV *pol-vpr* region. The deletion variant satisfied the requirements for a DIP. By introducing additional deletions to ablate splicing and eliminate expression from all HIV reading frames and repairing the HIV central polypurine tract, the DIP was engineered into an $R_0 > 1$ TIP that durably suppressed HIV replication in vitro and in humanized mice. The TIP also established latency and suppressed HIV rebound or outgrowth in vitro, including from patient cells, and after interruption of antiretroviral therapy. To test TIP efficacy in a physiological model, an analog TIP lentiviral vector was constructed for SIV. Infant rhesus macaques were administered the SIV TIP by a single intravenous (IV) injection, challenged with a highly pathogenic SHIV (SF162P3) through the IV route (24 hours later), and followed for ~30 weeks. TIP intervention durably suppressed SHIV viral load by $4\log_{10}$ in plasma and lymph tissue and resulted in significant reduction in disease. As predicted, TIPs conditionally replicated in vivo for >6 months, and TIP-treated animals exhibited significantly improved immune responses, and no evidence of increased inflammation. Full-length sequencing of SHIV revealed no evidence of increased evolution, recombination, or escape.

CONCLUSION: Epidemiological analyses argue that each 1log reduction in HIV viral load results in significant delays in the onset of AIDS and significant reductions in transmission potential. Theories have proposed that $R_0 > 1$ TIPs have the capacity to establish coevolutionary arms races with wild-type viruses, leading to extraordinarily high genetic barriers to the evolution of antiviral resistance. On the basis of TIP intervention in SHIV-infected rhesus macaques, mathematical modeling indicates that a single dose of TIPs could durably reduce HIV viral load to less than the World Health Organization threshold for HIV transmission of 10^3 copies/ml. These data suggest that TIPs could serve as the foundation for a new class of easy-to-administer, single-administration antiviral "drive" therapies. ■

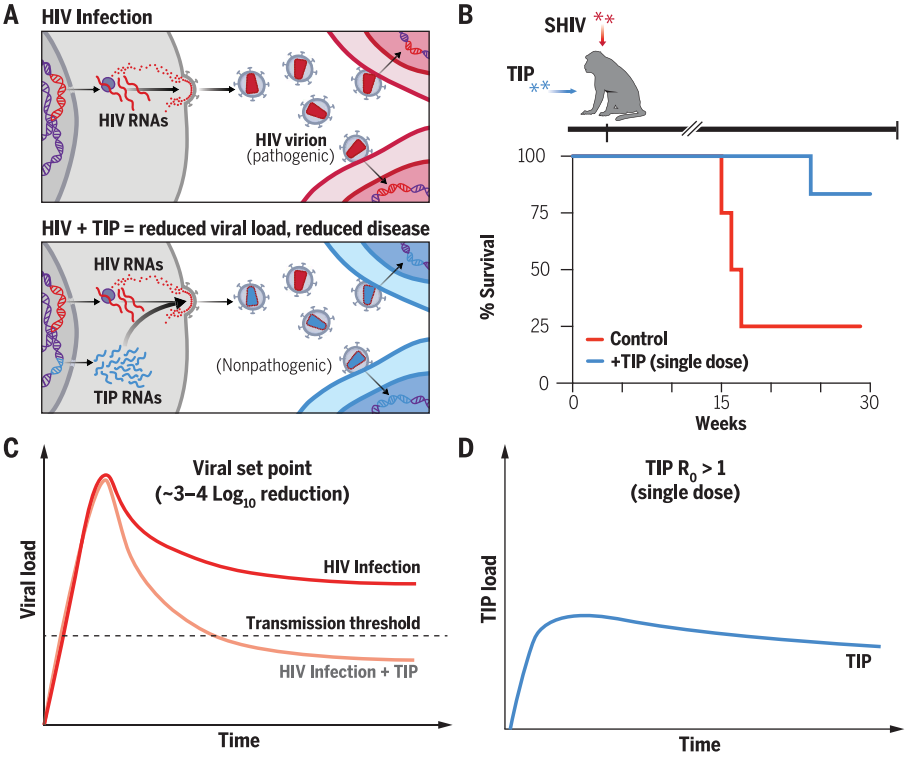

A single-dose HIV therapy: TIPs reduce disease in nonhuman primates through conditional replication. (**A**) Overview of the TIP concept. (**B**) TIP intervention in rhesus macaques infected with a highly pathogenic SHIV results in significant protection from disease. (**C** and **D**) TIP intervention durably reduces SHIV viral load by ~$4\log_{10}$ (C) owing to sustained conditional replication of TIPs (D).

The list of author affiliations is available in the full article online.
*Corresponding author. Email: leor.weinberger@ucsf.edu
†These authors contributed equally to this work.
Cite this article as F. N. N. Pitchai *et al.*, *Science* **385**, eadn5866 (2024). DOI: 10.1126/science.adn5866

READ THE FULL ARTICLE AT
https://doi.org/10.1126/science.adn5866

RESEARCH ARTICLE

HIV

Engineered deletions of HIV replicate conditionally to reduce disease in nonhuman primates

Fathima N. Nagoor Pitchai[1,2]†, Elizabeth J. Tanner[1,2]†, Neha Khetan[1,2], Gustavo Vasen[1,2], Clara Levrel[1,2], Arjun J. Kumar[1,2,3], Shilpi Pandey[4], Tracy Ordonez[4], Philip Barnette[4], David Spencer[4,5], Seung-Yong Jung[1], Joshua Glazier[1], Cassandra Thompson[1,6], Alicia Harvey-Vera[7,8], Hye-In Son[1], Steffanie A. Strathdee[7], Leo Holguin[7], Ryan Urak[9], John Burnett[9,10], William Burgess[11], Kathleen Busman-Sahay[11], Jacob D. Estes[11,12,13], Ann Hessell[4], Christine M. Fennessey[14], Brandon F. Keele[14], Nancy L. Haigwood[4], Leor S. Weinberger[1,2,15,16]*‡

Antiviral therapies with reduced frequencies of administration and high barriers to resistance remain a major goal. For HIV, theories have proposed that viral-deletion variants, which conditionally replicate with a basic reproductive ratio [R_0] > 1 (termed "therapeutic interfering particles" or "TIPs"), could parasitize wild-type virus to constitute single-administration, escape-resistant antiviral therapies. We report the engineering of a TIP that, in rhesus macaques, reduces viremia of a highly pathogenic model of HIV by >3$\log_{10}$ following a single intravenous injection. Animal lifespan was significantly extended, TIPs conditionally replicated and were continually detected for >6 months, and sequencing data showed no evidence of viral escape. A single TIP injection also suppressed virus replication in humanized mice and cells from persons living with HIV. These data provide proof of concept for a potential new class of single-administration antiviral therapies.

More than 39 million people currently live with HIV-1 or AIDS (hereafter referred to as HIV), and ~1 to 2 million new HIV infections occur each year, with the virus overly impacting underprivileged and underserved communities (*1*). Combination antiretroviral therapy (ART) suppresses HIV replication, but ART is not curative and must be continually administered, as discontinuation almost invariably leads to rapid viral rebound (*2*, *3*). Epidemiological projections indicate that controlling the HIV-AIDS epidemic by using conventional approaches may be challenging owing to deployment, behavioral, and mutational barriers (*4*–*6*). Consequently, single-administration therapeutics based on defective interfering particles (DIPs) have been proposed to overcome these barriers (*7*–*10*). Originally observed for influenza virus in the 1940s by von Magnus (*11*), DIPs are viral deletion mutants that conditionally replicate (i.e., lack self-replication) and act as molecular parasites of the wild-type virus within infected cells, stealing essential viral proteins (e.g., replication or packaging proteins) to reduce the levels of wild-type virus. Theoretical models predicted that DIPs could be engineered into long-acting, single-administration HIV therapies (termed "therapeutic interfering particles" or "TIPs"), provided that a basic reproductive ratio [R_0] > 1 (*7*, *8*) could be achieved (fig. S1, A and B). R_0 is a threshold value, defined as the expected number of secondary infections arising from a single infected individual or cell (*12*), and proof-of-concept R_0 > 1 TIPs were recently shown to be therapeutic in the context of acute, self-limiting infection (*13*, *14*). However, the concept's ultimate therapeutic promise is for chronic infections with high genetic variability, such as HIV, for which there is no available vaccine. Unfortunately, bona fide retroviral DIPs (the requisite chassis for TIPs) have remained elusive (*15*–*20*), and it was unclear if viable R_0 > 1 TIPs could be engineered for HIV, whether they would be therapeutic in the chronic setting, or whether efficacy could be sustained given HIV's high genetic variability.

Results

Isolation of an HIV DIP

To first understand why DIPs have been elusive for lentiviruses, despite DIPs being readily isolated for other RNA viruses (*11*, *21*) and the abundance of defective HIV genomes (*22*, *23*), we used established in silico models of HIV (*24*, *25*), which predicted that spontaneously generated DIPs would not expand in conventional serial-passage cultures as a result of dilution effects. The models further predicted that 50 to 100 days of nondilutive culturing would be required for a DIP to reach detectable levels (fig. S1C). Accordingly, we developed a nondilutive continuous-culture reactor (fig. S1, D and E) in which $CD4^+$ target cells were replenished exclusively by cell division for up to 100 days. The reactor was infected with a green fluorescent protein (GFP)–expressing HIV (*26*), von Magnus–like fluctuations (*27*) were observed (Fig. 1A), and after ~100 days of culture, remaining GFP^+ cells were isolated, and the viral DNA was sequenced. Proviral DNA analysis revealed a ~2.5-kb deletion in the HIV *pol-vpr* region (Fig. 1A), which resulted in the complete deletion of ribonuclease H, integrase, and the truncation of reverse transcriptase. A similar deletion arose in a parallel reactor, and, in both cases, the deletions were flanked by short identity regions, suggesting recombination events (fig. S1F).

To test whether the ~2.5-kb deletion generated a DIP (fig. S1B), the deletion was cloned into HIV (right, Fig. 1A); the construct also encoded a long terminal repeat (LTR)–driven GFP reporter and a nonfunctional Tat protein, necessitating HIV superinfection to transactivate its expression (fig. S2, A and B). Firstly, to test for conditional replication, we verified that the deletion variant could only produce transduction-competent viral-like particles (VLPs) conditionally upon rescue (i.e., complementation in trans) with the deleted HIV proteins (Fig. 1B). Secondly, we quantified the deletion variant's ability to interfere with HIV production; in single-round infections, the deletion variant reduced HIV titers by 94% ($P = 5 \times 10^{-6}$) (inset, Fig. 1C, and fig. S2C). Notably, cells with an integrated copy of the deletion variant were equally as permissive to incoming HIV infection in the first round as control cells without an integrated deletion variant (fig. S2C), and control GFP-expressing HIV-derived lentiviral vectors (fig. S3, A and B) generated no interference, indicating that the data cannot be explained by resistance to infection. Interference was further verified in alternate cell lines (fig. S4A) as well as in donor-derived human primary $CD4^+$ T cells (fig. S4, B and C). Thirdly, to test whether the deletion variant mobilized in the presence of replication-competent HIV (e.g., through stealing packaging proteins from HIV), RNA was quantified in extracellular VLPs. Of the extracellular RNA, 60% was from the deletion variant, indicating a packaging advantage for the variant over HIV (Fig. 1D, left). These data verify that the deletion variant constitutes a bona fide DIP by (i) conditionally replicating only in the presence of HIV,

[1]Gladstone Center for Cell Circuitry, University of California, San Francisco, CA, USA. [2]Gladstone Institute of Virology, University of California, San Francisco, CA, USA. [3]Department of Bioengineering, University of Washington, Seattle, WA, USA. [4]Oregon National Primate Research Center, Oregon Health & Science University, Beaverton, OR, USA. [5]Absci Corporation, Vancouver, WA, USA. [6]Department of Molecular Microbiology, Washington University School of Medicine, St. Louis, MO, USA. [7]Global Health Sciences, Department of Medicine, University of California San Diego, La Jolla, CA, USA. [8]US-Mexico Border Health Commission, Tijuana, Mexico. [9]Center for Gene Therapy, Beckman Research Institute, City of Hope National Medical Center, Duarte, CA, USA. [10]Department of Microbiology and Immunology, Miller School of Medicine, University of Miami, Miami, FL, USA. [11]Vaccine and Gene Therapy Institute, Oregon Health & Science University, Beaverton, OR, USA. [12]Faculty of Health, Department of Clinical Medicine, Aarhus University, Aarhus, Denmark. [13]School of Health and Biomedical Sciences College of Science, Engineering and Health RMIT University, Melbourne, Australia. [14]AIDS and Cancer Virus Program, Frederick National Laboratory for Cancer Research, Frederick, MD, USA. [15]Department of Pharmaceutical Chemistry, University of California, San Francisco, San Francisco, CA, USA. [16]Department of Biochemistry and Biophysics, University of California, San Francisco, San Francisco, CA, USA.
***Corresponding author. Email: leor.weinberger@gmail.com**
†These authors contributed equally to this work.
‡Present address: Institute for Evolvable Medicines (IEM), Oakland, CA, USA.

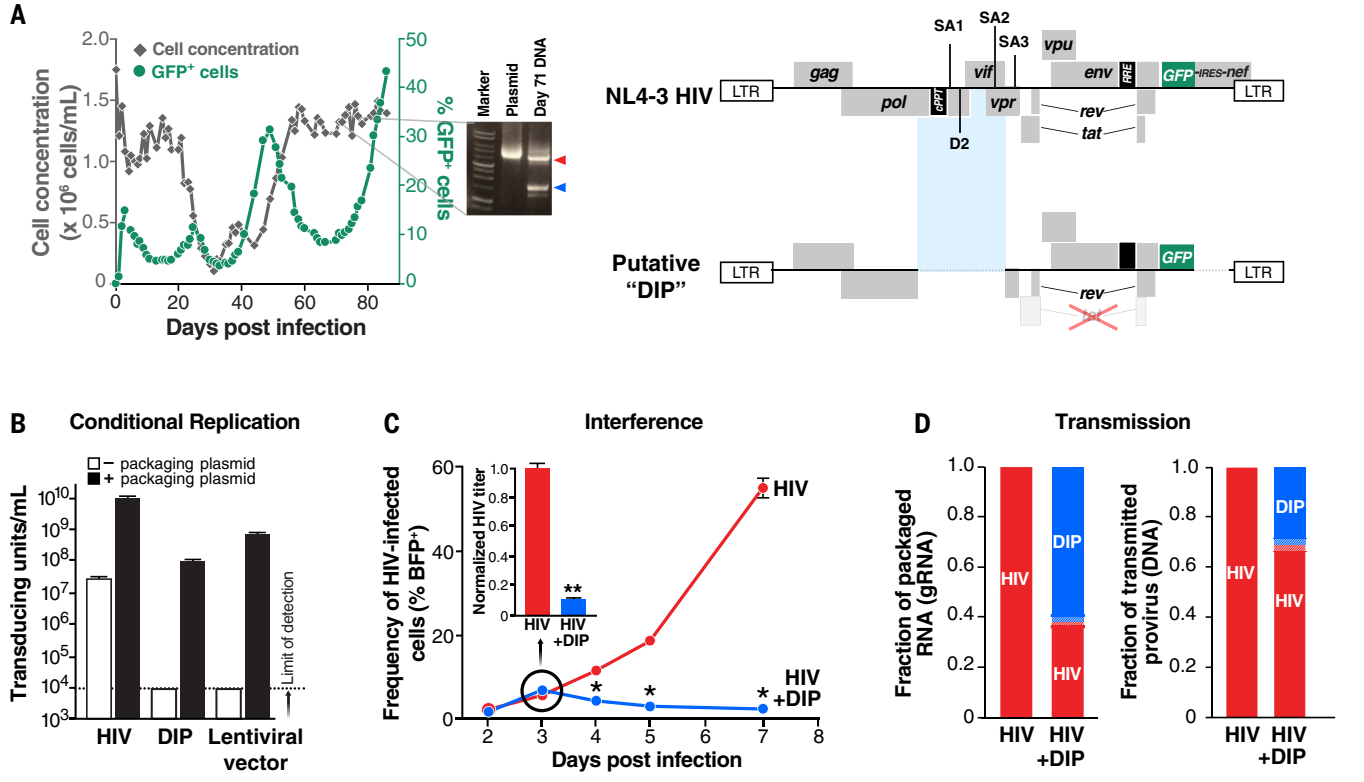

Fig. 1. Long-term selection of an HIV DIP. (**A**) Detection of an HIV deletion variant in a CEM cell bioreactor. (Left) Cell concentration and frequency of GFP$^+$ cells by flow cytometry in a long-term bioreactor infected with replication-competent HIV-GFP (*26*). (Inset) PCR-amplified HIV proviral DNA from day 71 cells (lane 3: red arrowhead, expected band; blue arrowhead, ~2.5-kb deletion). (Right) Putative DIP construct with the location of the 2.5-kb deletion. D2, splice donor D2; SA, splice acceptor; IRES, internal ribosome entry site; RRE, Rev response element; nef, negative factor. (**B**) Conditional packaging assay: DIP VLPs were assembled in the presence or absence of lentiviral packaging plasmid, and transduced MT4 cells were titered by flow cytometry relative to a lentiviral GFP control vector. (**C**) Interference assay: HIV outgrowth in the presence or absence of the putative DIP. Cells stably transduced with single integrations of DIP or a mock-transduced control were infected with HIV-BFP, and the frequency of BFP$^+$ cells was measured by flow cytometry. (Inset) Filtered supernatants were harvested at 3 days postinfection (dpi) and titered by flow cytometry. *P = 0.004 (4 dpi); P = 0.001 (5 dpi); P = 0.001 (7 dpi); **$P = 5 \times 10^{-6}$; Student's t test. (**D**) Transmission assay: The fraction of putative DIP or HIV genomic RNA in supernatant VLPs (left) compared with the fraction of proviral DNA integrated in downstream transduced cells (right) at 3 dpi.

(ii) interfering with HIV outgrowth, and (iii) mobilizing from infected cells.

Engineering the DIP into an $R_0 > 1$ TIP

Previous theoretical modeling (*7*, *8*) stipulated that for a DIP to constitute a TIP, it must conditionally mobilize with $R_0 > 1$. However, in subsequent rounds of infection, the DIP accounted for only 30% of integrated provirus (Fig. 1D, right), indicating $R_0 < 1$. We hypothesized that poor DIP transmission could be due to loss of the central polypurine tract (cPPT), contained within the 2.5-kb deleted region, which enhances transduction efficiency (*28*–*32*) and appears critical for efficient $R_0 > 1$ transmission (*33*). To rationally enhance DIP transmission efficiency, the cPPT was reintroduced back into the deletion variant (Fig. 2A), which generated a twofold increase in VLP transduction efficiency (Fig. 2B). Further optimization to ablate additional protein expression (tat, rev, vpu, and env) enhanced transmission further (Fig. 2B and table S1). These engineered constructs (putative TIP-1 and TIP-2; table S1) retained DIP properties, including conditional replication, packaging, and interference (Fig. 2C and fig. S5, A to C), and generated significant interference in donor-derived human primary CD4$^+$ cells (Fig. 2D), thereby constituting putative TIPs.

To directly measure the TIP-specific R_0 (R_0^{TIP}), a three-color assay was developed (Fig. 2E and fig. S6A), wherein cells were stably transduced with a single copy of TIP (encoding a GFP reporter), infected with full-length HIV [blue fluorescent protein (BFP)–tagged] to become "producer" cells, and subsequently cocultured with an excess of susceptible mCherry$^+$ "target" cells. The assay quantified single-round HIV and TIP transmission into target cells from the fractions of double-positive BFP$^+$-mCherry$^+$ and GFP$^+$-mCherry$^+$ cells, respectively (e.g., double-positive GFP$^+$-mCherry$^+$ cells indicated TIP transmission from producer to target cells, with the fraction of double positives allowing calculation of R_0^{TIP}). To test whether the assay yielded physiologically relevant R_0 values, the R_0 of HIV alone was measured (i.e., in the absence of TIP) and found to be $R_0^{HIV} = 24$, consistent with upper estimates of the HIV R_0 in vivo (*25*, *34*, *35*). In parallel, the assay yielded an $R_0^{TIP} = 12$ (Fig. 2F). To verify $R_0^{TIP} > 1$, we quantified the initial slope of TIP expansion relative to an expanding HIV infection (i.e., $R_0^{HIV} > 1$); TIPs exhibited substantial transmission into target cells, showing an exponential rate of increase ~sixfold faster than HIV over multiple rounds of infection (Fig. 2G). Notably, TIP-transduced cells did not show altered survival (either enhanced or diminished) compared with infected, mock-transduced cells (fig. S6, B and C), indicating that TIP expansion is not the result of purifying selection. Also consistent with the $R_0 > 1$ mechanism, in multiweek reactor cultures, the TIP significantly and durably reduced HIV viral loads, protecting cultures from exponential HIV growth for at least 40 days (Fig. 2C). In further support of the $R_0 > 1$ mechanism of interference, deletion of the TIP packaging signal (Ψ) (*36*) significantly blunted the interference effect by ~30% (Fig. 2H and fig. S7, A and B), as expected from the partial penetrance of the Ψ packaging signal

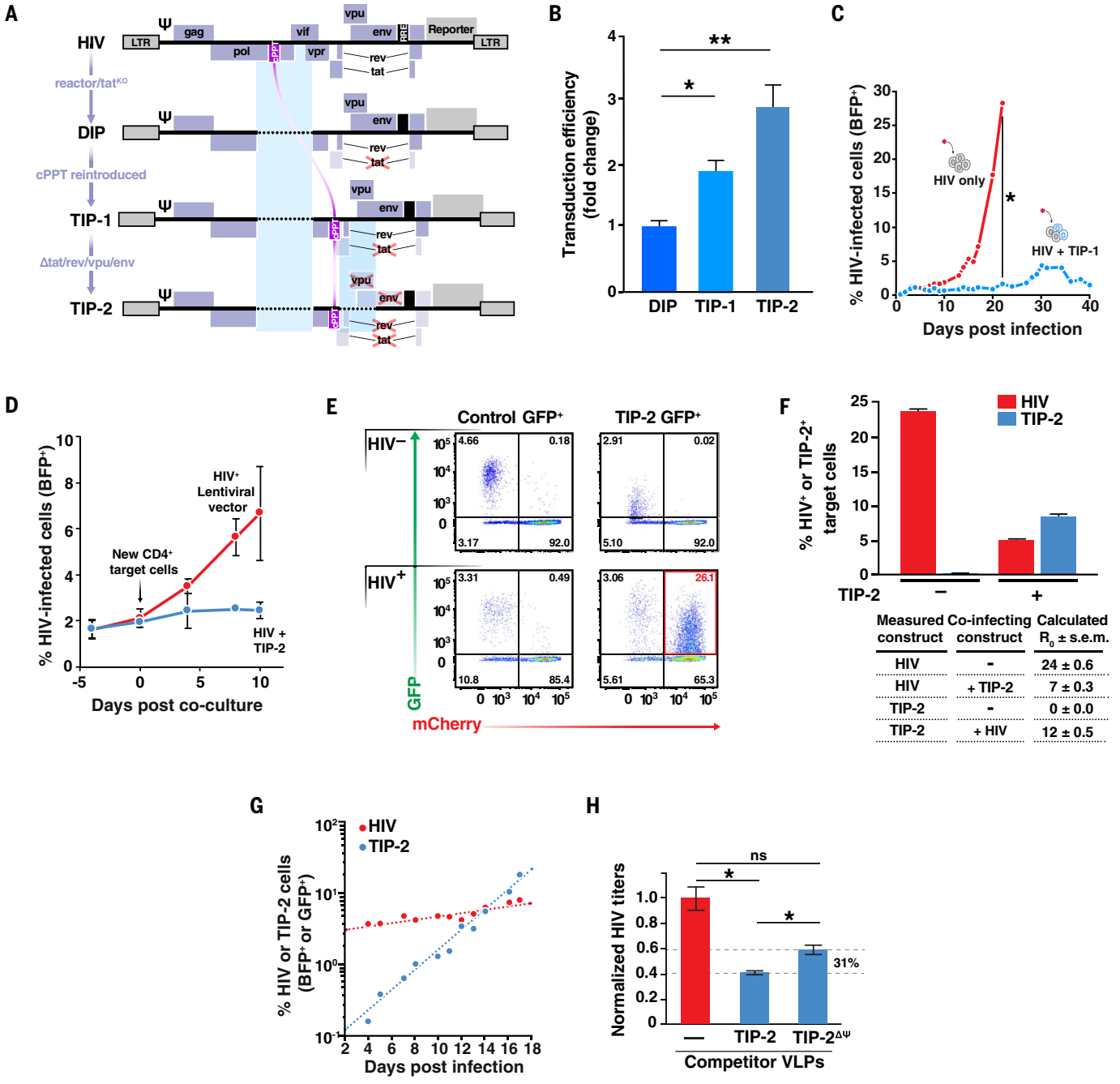

Fig. 2. Engineering the HIV TIP. (**A**) Schematics of full-length HIV, DIP, and engineered TIP constructs; the cPPT was reintroduced in "TIP-1," and additional coding sequences were ablated in "TIP-2" to reduce extraneous HIV protein expression (table S1). KO, knockout. (**B**) Transduction efficiencies of DIP, TIP-1, and TIP-2 VLPs (normalized to p24 capsid protein and assayed on MT-4 cells; mean of three biological replicates shown). *P = 0.007 and **P = 0.003 from Student's t test. (**C**) TIP interference: Frequency of HIV-infected cells during long-term culture in the presence or absence of TIP-1–transduced cells. Cultures were seeded at a ratio of 1:1 of untransduced and TIP-1–transduced cells (the construct used, TIP-1/Δenv, has an additional *env* mutation; see table S1), infected with HIV-BFP, and monitored by flow cytometry. *P < 0.0006 from Student's t test. (**D**) TIP-2 interference in donor-derived human CD4$^+$ primary cells; 50% of cells were transduced with TIP-2 or lentiviral GFP control (*33*) infected with HIV-BFP, and new activated target cells were added. HIV-BFP$^+$ cells were quantified by flow cytometry (mean ± SD of two biological replicates is shown). (**E**) Cells from the three-color assay were analyzed by flow cytometry 3 days post coculture to quantify mobilization of TIP (or control) from "producer" cells into mCherry$^+$ "target" cells conditional on HIV (see red box for dual positives). (**F**) Measured R_0 values (mean ± SEM of three biological replicates). (**G**) Relative TIP R_0 by transmission in culture. Reactor was seeded with excess (~87%) target CEMs (mCherry$^+$) and ~13% TIP-2 (GFP$^+$), infected with HIV-BFP, and assayed by flow cytometry for double-positive BFP-mCherry$^+$ and GFP-mCherry$^+$ cells. Trendlines fit to HIV or TIP-2 viral loads [i.e., $V.L.(t) = Ce^{rt}$, where r represents growth rate and C represents the initial viral load], and best-fit values are r_{TIP} = 0.33 and r_{HIV} = 0.054. (**H**) Quantification of interference from TIP packaging: TIP-2– or TIP-2$^{\Delta\Psi}$–transduced cells were infected with HIV-BFP, the supernatant was collected at 2 dpi, and levels of integration-competent HIV were titered in target cells by flow cytometry (mean ± SEM of three biological replicates; ns, nonsignificant; *P < 0.01; Student's t test).

(*37*) and consistent with TIP RNAs competing intracellularly for viral Gag polyprotein precursor (*7*, *8*, *10*).

In vivo analysis of TIP efficacy

To test TIP efficacy in vivo, we first performed pilot studies in two humanized mouse models, the peripheral blood mononuclear cell (PBMC) NSG mouse model (*38*) and the longer-duration CD34$^+$ NSG model (*39*), commonly used for preclinical evaluation of new HIV antiviral candidates (*40*, *41*). In these models, immunodeficient (NSG) mice, engrafted with either human CD4$^+$ T cells or CD34$^+$ progenitor cells, were infected with HIV and subsequently administered TIP lentiviral vector through direct intravenous (IV) injection 5 days following HIV challenge to evaluate TIP efficacy after a single-injection administration (fig. S8A). For these in vivo studies, we attempted to optimize the HIV TIP candidate first by ablating its Gag expression through a frameshift in *gag-pol*, which unfortunately blunted TIP interference (fig. S8B). Consequently, we instead incorporated two smaller deletions identified in a recent library screen (*33*)—one in the 5′ end of *gag* that allows ~100 amino acids of Gag to be expressed and the other in the 3′ end of *env* (fig. S8C and table S1)—both of which led to enhanced TIP efficacy (fig. S8D). In both mouse models, HIV TIP treatment generated significant reductions in HIV viral load (Fig. 3A and fig. S8E). The reduction in HIV viral load was still apparent when viremia was normalized to CD4$^+$ T cell counts, indicating that the effect could not be explained by target-cell depletion (fig. S8, F and G).

To more definitively evaluate in vivo efficacy, we used a highly pathogenic simian immunodeficiency virus (SIV) nonhuman primate (NHP) model (fig. S9A), where infant rhesus macaques are infected with the recombinant virus SHIV-SF162P3 (an SIVmac239 virus encoding HIV *env*) (*42*–*44*). This infant NHP model exhibited exceptionally rapid progression to an AIDS-like disease and clinical endpoint with a 50% survival time of ~15 weeks (Fig. 3B). As in previous immune-therapy studies in this model (*42*–*44*), animals were administered the intervention 24 hours prior to virus challenge. Notably, this intervention schedule mimics the likely clinical testing scenario—i.e., analytical treatment interruption (ATI), where antiviral candidates are administered prior to viral rebound—as pre–steady state viral kinetics during early acute infection closely approximate viral rebound kinetics following ATI (*2*, *3*).

Testing in the NHP model required development of an analog SIV TIP based on SIVmac239 (fig. S8C and table S1). The analog SIV TIP (pseudotyped with SIV *env*) was first tested in vitro to verify its ability to suppress viral outgrowth in primary rhesus splenocytes (fig. S9, B to D). Then, infant rhesus macaques were administered the SIV TIP [3 ml of ~10^7 transducing units (TU)/ml] through a single IV injection, challenged with SHIV-SF162P3 (100 IU) through the IV route (24 hours later), and followed for ~30 weeks (~7 months) or until clinical endpoint (fig. S9A). Similar to historical controls, infected (untreated) animals exhibited rapid pathogenesis (Fig. 3B). Notably, Kaplan-Meier survival analysis showed that TIP-treated animals exhibited a significant survival advantage (Fig. 3B) with no observable outward signs of simian AIDS or gross pathogenesis before the scheduled study termination at 30 weeks postinfection except for one TIP-treated outlier animal that reached clinical endpoint at 24 weeks.

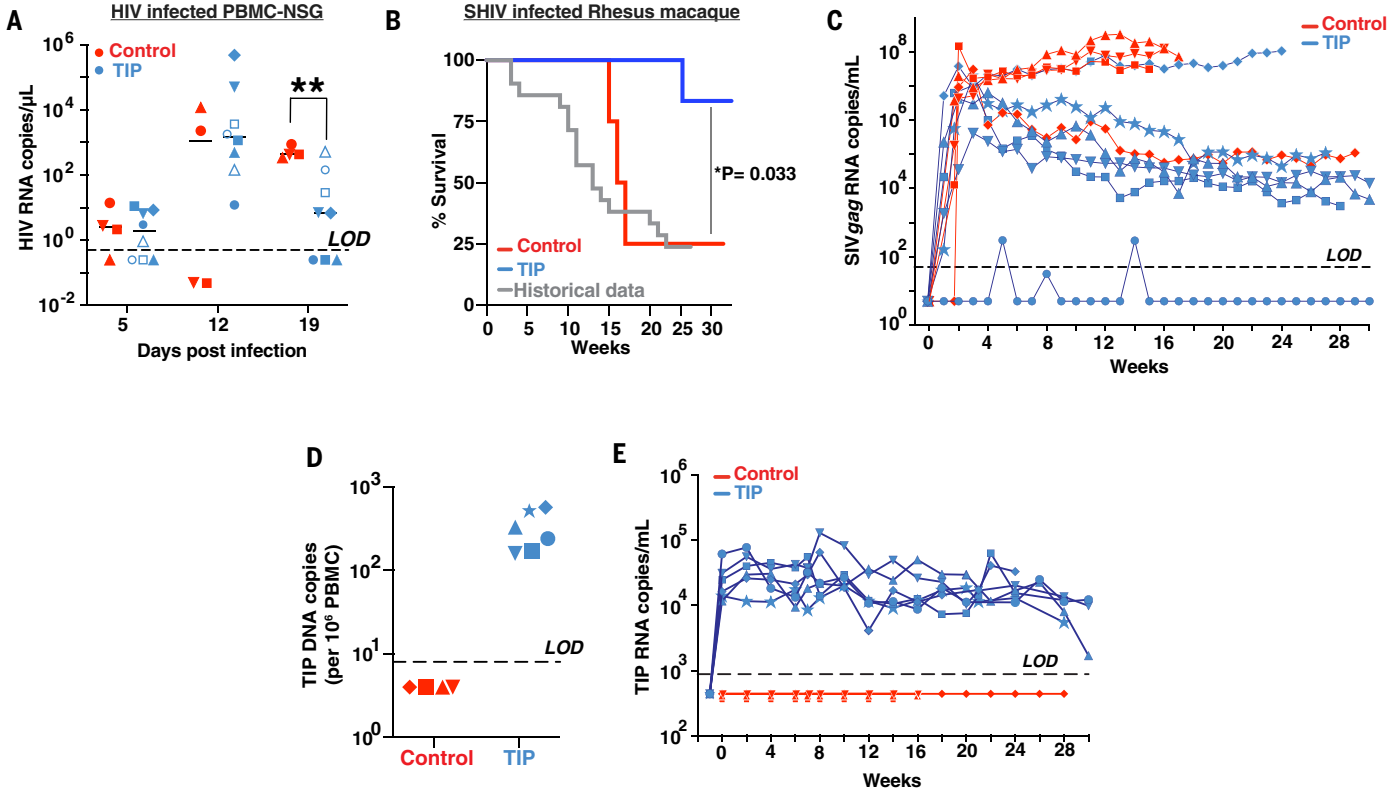

Fig. 3. TIP intervention in humanized mice and rhesus macaques. (**A**) Human PBMC model: NSG mice were engrafted with human cells, challenged with HIV, and then administered a single IV injection of HIV TIPs (~10^6 TU/kg) or mock at 5 days postinfection. HIV RNA plasma viral loads in NSG mice treated with TIP (n = 8) or HIV (control; n = 4) at days 5, 12, and 19 post HIV infection. **P = 0.005. LOD, limit of detection. (**B**) Rhesus macaque model: Kaplan-Meier survival analysis of TIP-treated animals (blue, n = 6) compared with controls (red, n = 4) [Log-rank (Mantel-Cox) test] and historical controls (gray, n = 21). (**C**) Quantitative PCR of SIV viral RNA (SIV *gag*) in peripheral blood plasma; Blue = TIP-treated animals, red = control animals (each animal represented by a unique symbol). (**D**) Reverse-transcribed TIP DNA in peripheral blood mononuclear cells from day 1 post TIP intervention. (**E**) Quantitative PCR of TIP RNA copies in peripheral blood plasma.

Reverse transcription quantitative polymerase chain reaction (RT-qPCR) analysis of viral loads in peripheral blood plasma (Fig. 3C) showed that almost all animals reached peak viremia of ~10^7 copies/mL at 2 weeks post-infection. Subsequently, three of four untreated animals established set-point viral loads of ~10^8 copies/mL, consistent with previous reports (*45*, *46*). By contrast, five of six TIP-treated animals exhibited dramatic reductions in set-point viral load, settling at ~10^4 SHIV RNA copies/mL, and one TIP-treated animal exhibited extremely low, intermittent viral load (i.e., a ~3$\log_{10}$ to 5$\log_{10}$ reduction). In these TIP-treated animals, the set-point reduction was durable and maintained for the duration of the 30-week study.

Following TIP injection, reverse-transcribed TIP DNA was robustly detected in the PBMCs of TIP-treated animals (Fig. 3D). As opposed to humans, in which longitudinal analysis of integrated proviral DNA is standard, in rhesus macaques, such analysis is exceptionally technically challenging (*47*), in part owing to their smaller size, which limits the number of $CD4^+$ T cells that can be collected during a blood draw. However, consistent with $R_0^{TIP} > 1$, extracellular TIP RNA was robustly detected in the blood plasma of TIP-treated animals (at 10^4 to 10^5 copies/mL) throughout the entire 30-week study (Fig. 3E) despite the single administration of TIPs. Assay specificity was confirmed by testing control animals for TIP, and neither TIP DNA nor RNA were detected in untreated, HIV-infected animals (Fig. 3, D and E).

To physiologically assay the immune health of the animals, we used an established approach (*42*–*44*) that tests for the ability to mount an adaptive immune response (i.e., seroconversion) to the Env protein. The inability of animals to seroconvert is characteristic of loss of immune function as a result of viral pathogenesis (i.e., high viremia leading to rapid progression to AIDS). As expected, untreated animals exhibited poor seroconversion, inversely correlated with viral load, consistent with the less-developed immune systems of these infants (*44*). By contrast, TIP-treated animals exhibited greatly improved seroconversion (Fig. 4A), concordant with their reduced viral loads. $CD4^+$ T cell levels exhibited modest declines in both TIP-treated and untreated animals (fig. S9, E and F), in agreement with previous findings that $CD4^+$ T cell levels have limited correlation with disease progression (*48*–*54*).

To determine whether plasma viremia was representative of viral replication in lymphoid tissue, where the majority of viral replication occurs, we assessed SHIV RNA in lymph nodes through quantitative spatial imaging, i.e., RNAscope in situ hybridization (*55*, *56*) (Fig. 4B and fig. S10, A to H). SHIV RNA in lymph nodes of TIP-treated animals was substantially reduced compared to untreated animals and, across all animals, there was high correlation ($R^2 = 0.89$) between SHIV levels within lymph nodes and peripheral blood plasma (Fig. 4C) as well as SHIV proviral DNA levels in lymphoid cells (fig. S10I).

To rule out alternate mechanisms of action, we examined full-length SHIV sequences and viral kinetics in the animals. To test the hypothesis that reduced SHIV viral loads could be due to evolutionary selection for an attenuated SHIV variant, full-length SHIV sequencing was performed from endpoint samples of all animals. No large deletions or rearrangements were detected in SHIV RNA (fig. S11) (GenBank accession nos. PP597405 to PP597522) or proviral DNA (GenBank accession nos. PP646066 to PP646153), and the majority of evolution (i.e., single-nucleotide polymorphisms) was observed in *env*, consistent with lifetime extension of TIP-treated animals enabling more viral replication as well as immune pressure from seroconversion (fig. S12). Because one animal (40471, figs. S11 and S12) exhibited a longer branch than others, we performed full-length alignment analysis with the parental molecular clone but did not observe evidence of recombination (data S1).

To test the hypothesis that TIP intervention may have reduced the effective SHIV inoculum, we analyzed viral load kinetics using an established analytic approach in which the viral peak/set point ratio (*57*–*59*) is exploited to discriminate underlying physiological mechanisms. As expected, the basic model of in vivo viral dynamics (*24*, *25*) was sufficient to fit viral kinetics in untreated animals (Fig. 4, D and E, and fig. S13), but not TIP-treated animals (under any parameter combinations), consistent with reports (*58*, *59*) that fitting peak/set point ratios of ~10-fold or greater require mechanisms that dynamically respond to viral load. Notably, the similar magnitude and timing of peak viremia levels between TIP-treated and untreated groups (Fig. 3C) is inconsistent with the results being explained by a reduced SHIV inoculum in the TIP-treated group. Moreover, no evidence of an increased inflammatory response, which correlates with more rapid disease progression in rhesus macaques (*60*) and people living with HIV who are long-term nonprogressors (*61*), was detected in TIP-treated animals (fig. S14), further suggesting that static innate mechanisms cannot explain the reduced viral loads in TIP-treated animals. Notably, an extension of the basic viral dynamics model incorporating TIPs (*7*), which dynamically respond to viral load as obligate molecular parasites, was sufficient to fit the viral kinetics of TIP-treated animals (Fig. 4, D and E, and fig. S15A). The modeling indicated that the single nonresponding TIP-treated animal exhibited substantially higher T cell turnover, consistent with previous predictions that such increased turnover could limit TIP efficacy (*7*). The measured in vivo viral set-point viral load matched analytically predicted steady state viremia levels, suggesting early and durable establishment of the viral set point in TIP-treated animals and that longer-term studies would yield little added viral kinetics information (fig. S15B).

Extrapolating efficacy of HIV TIPs to the human context

We next asked whether TIPs could provide any benefit in the context of viral latency, given the noncurative nature of ART. Our previous studies argued that lentiviral vectors obligately establish latency and will reverse latency when Tat is delivered in trans (*62*–*64*). Thus, we hypothesized that TIP-transduced cells would survive under ART and would reverse latency together with HIV upon interruption of ART to thereby suppress HIV outgrowth. On the basis of established latency quantification protocols (*65*), we developed an in vitro viral outgrowth assay (fig. S16A). We found that TIP genomes were maintained for at least 26 days under ART (Fig. 5A and fig. S16B), and upon ART cessation, TIPs rebounded with HIV significantly interfering with HIV outgrowth (Fig. 5, B and C) and protecting cells from cytopathic effects (fig. S16C).

We quantified TIP antiviral efficacy in human donor–derived primary T lymphocytes (fig. S16D). Briefly, activated primary $CD4^+$ T cells were transduced with TIP or a control vector, infected with HIV, and then followed for 21 days through coculture with additional T cell targets. As in previous studies (*39*, *66*–*70*), HIV infection level was indirectly quantified by depletion of CD4 cells (Fig. 5, D and E), and depletion was consistent with similar humanized animal models (*71*, *72*). HIV-TIP transduction protected the CD4 population, whereas TIPs appeared to be maintained both in terms of GFP-reporter expression (Fig. 5D) and genomic DNA (Fig. 5F). HIV-TIP transduction did not substantially affect proliferation of primary $CD4^+$ T cells, and cell expansion was consistent with protection from HIV killing (fig. S16E).

We also quantified integrated TIP antiviral efficacy on samples from donors living with HIV (fig. S17A). Since the most likely clinical use scenario for TIP intervention would be to benefit individuals in resource-limited settings who cannot access ART long term, PBMCs were obtained from untreated persons living with HIV. To stimulate HIV outgrowth, PBMCs were cocultured with $CD4^+$ target cells transduced with TIPs or a control GFP vector. TIP treatment significantly reduced HIV outgrowth compared with the control vector (fig. S17A), suggesting that TIP intervention can be effective against patient-derived viruses.

Because SIV and SHIV in rhesus macaques produces viral loads that are higher than those in HIV-infected humans (i.e., 10^7 to 10^8 copies/mL

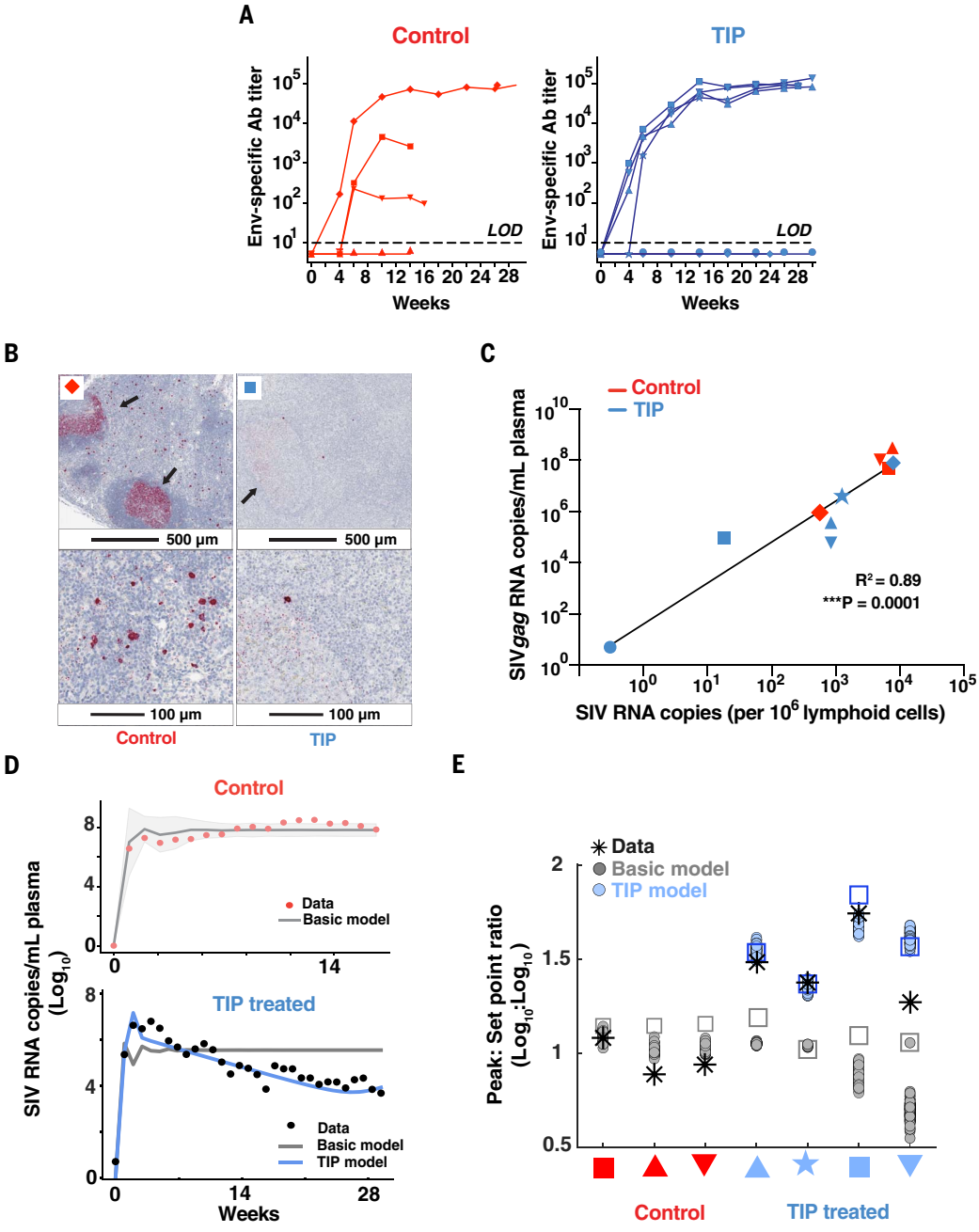

Fig. 4. Immune response, in situ tissue analysis, and quantitative modeling of SHIV kinetics. (**A**) Seroconversion ability of TIP-treated versus control animals (ELISA for HIV Env). (**B**) Representative images of SHIV RNA expression within lymphoid tissue by RNAscope in situ hybridization (top scale bar, 500 µm; bottom scale bar, 100 µm). (**C**) Correlation between qPCR of SIV *gag* RNA in plasma and the quantified proportion of SHIV RNA$^+$ cells within lymph nodes from RNAscope. ****P = 0.0001. (**D**) Best fits (nonlinear least-squares regression) of mathematical models to SHIV viral load data from a representative control animal (top) and TIP-treated animal (bottom). Data from control animals were fit to the basic ODE model (gray), whereas data from TIP-treated animals fit to both the basic model and TIP model (blue). (**E**) Model fitting summary: Ratio of peak to steady-state SHIV viral load data (* symbol) together with mathematical model fits from Markov chain Monte Carlo sampling (○ symbol) and the best fits from Latin-Hypercube sampling (□ symbol). Gray symbols represent the basic model of viral dynamics, whereas blue symbols represent the model with TIPs incorporated.

in rhesus macaques versus 10^4 to 10^5 copies/mL in humans), we asked what effect HIV TIPs might have given the lower HIV set point in humans. To predict the magnitude of HIV set point reduction in humans, we parametrized established mathematical models based on the NHP data. The resulting simulations indicated that TIPs could generate a $2\log_{10}$ to $3\log_{10}$ reduction in HIV set point in humans, resulting in viral loads $<10^3$ copies/mL (Fig. 5G), which could substantially reduce viral transmission (*8*, *73*). Overall, these results suggest that TIPs could represent a single-administration HIV therapeutic with the potential to limit viral burden and consequently reduce viral transmission below the World Health Organization–defined transmission threshold (*74*).

Mechanistically, how TIPs achieve $R_0 > 1$ in vivo given that only a minority of target cells (~1%) are productively HIV infected at any given time during set point viremia (*25*, *75*) is best explained by standard viral dynamical models and established recombination frequencies (*76*, *77*). These mathematical models (*24*) indicate that the rapid turnover of HIV-infected CD4$^+$ T cells exposes a substantial fraction of cells to HIV infection within a few weeks, and thus, CD4$^+$ T cells with TIP integrations have a substantial probability of being superinfected by HIV (*7*–*10*). The models are consistent with observations that 5 to 10% of infected cells harbor multiple proviral integrations during chronic HIV infection (*78*) and reported high in vivo recombination rates observed for HIV (*76*, *77*). Also in agreement with these models, previous gene therapy strategies that were dependent on HIV superinfection of vector-integrated T cells temporarily reduced viral load in clinical trials (*16*), although the therapeutic effect diminished over time owing to a lack of vector persistence (i.e., $R_0 < 1$) (*79*).

Although no immunotoxicity from TIP intervention was observed in NHPs, it is prudent

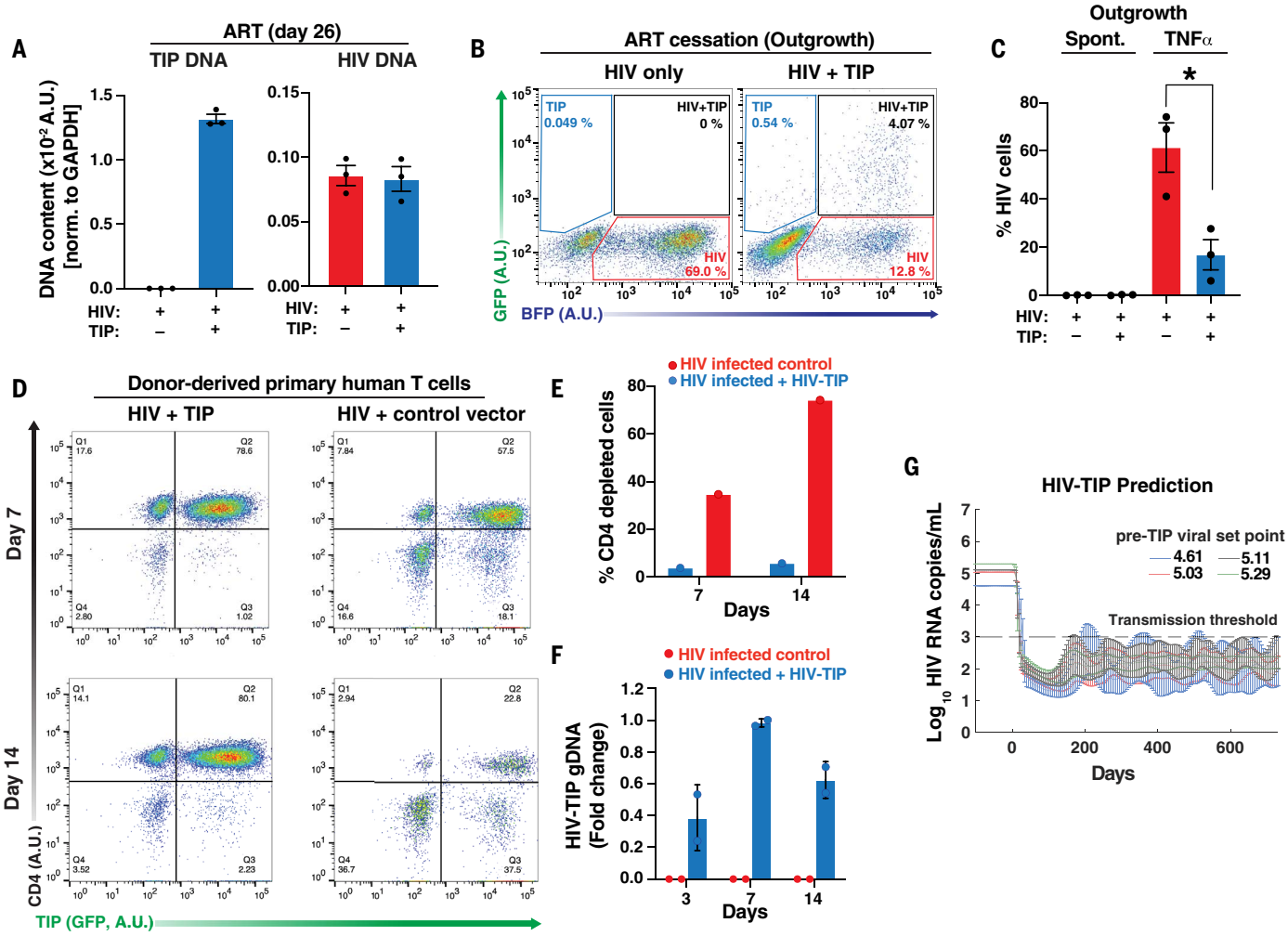

Fig. 5. Effects of TIPs on HIV latency reversal, CD4 protection, and extrapolation to human intervention. (**A**) Latency assay: qPCR quantification of integrated TIP DNA in Jurkat cells infected with HIV and/or transduced with TIP (optimized HIV-TIP, left). qPCR quantification of integrated HIV DNA (right) in cells infected with HIV and/or transduced with TIP during extended ART treatment (day 26) [normalized to glyceraldehyde-3-phosphate dehydrogenase (GAPDH)]. (**B**) Latency reversal upon ART cessation: fluorescence-activated cell sorting (FACS) analysis of Jurkat cells following ART cessation (+TNF-α) in the HIV control (left) versus TIP-treated samples (right). A.U., arbitrary units. (**C**) Percentage of HIV$^+$ cells reactivated spontaneously following ART cessation (background) and in presence of TNF-α in both the HIV control versus the TIP-treated sample. *P = 0.05. (**D**) CD4 protection assay: FACS analysis of human donor–derived primary CD4$^+$ T cells infected with HIV and transduced with either TIP (optimized HIV-TIP) or a control HIV-derived lentiviral vector, both expressing GFP. (**E**) HIV infection spread as assayed by CD4 depletion in the HIV-TIP– and control-treated samples on days 7 and 14. (**F**) qPCR quantification of integrated TIP DNA in donor-derived human primary CD4$^+$ T cells from days 3 to 14. (**G**) Predicted reduction in HIV set-point viral load following TIP intervention at physiological HIV set point values (based on model extrapolation from rhesus macaque data).

to consider potential TIP genotoxicity. Historically, lentiviral gene therapies that integrate in T cells have not been associated with increases in cancers (*79*–*81*), and HIV-associated B cell malignancies are known to result from T cell depletion rather than genotoxicity (*62*) except in very rare cases (*82*). However, a recent report (*83*) indicates 22 secondary CD8$^+$ T cell cancers in >27,000 chimeric antigen receptor (CAR) T cell–treated individuals. As that report notes, it remains unclear if these secondary cancers are due to lentiviral integration (in three cases, the CAR gene was detected in the malignant clone) or chemotherapy, and, notably, the incidence of secondary cancers following chemotherapy for lymphomas is substantially higher (*84*–*86*).

Although there have been reports of CD4$^+$ T cell cancers in persons living with HIV, there are at least two speculations as to why CD4$^+$ T cell cancers are rare in HIV-infected patients despite the extensive insertional mutagenesis in CD4$^+$ T cells evidenced by the large reservoir of defective proviruses (*22*, *65*): (i) These T cell cancers require the accumulation of multiple additional nonvirus induced mutations (*87*), or (ii) HIV's tropism to replicate in activated CD4$^+$ T cells may inherently target and control any transformed CD4$^+$ T cells. Although TIPs could sample more integration sites to increase the risk of transformation, they lack Tat transactivation likely required for LTR-driven transformation (*88*), and so the above speculations would likely still act to limit TIP-mediated expansion of transformed cells.

Recombination between HIV and TIPs (or extant defective proviruses) is also a potential concern but was not observed in plasma virus (fig. S11), perhaps because TIP internal deletions substantially reduce recombination efficiency (*10*). Notably, putative HIV-TIP recombinants could only be conditionally generated in the presence of replicating HIV, and, in the improbable extrema where TIPs regain

replication competence, these putative recombinants would be conceptually equivalent to conventional loss-of-efficacy mutations for therapeutics (*89*), i.e., consistent with equal or lower pathogenicity, assuming that the putative recombinant has equivalent tropism and equivalent drug, immune, and interferon sensitivities.

Evolutionarily, it is unclear why HIV DIPs or TIPs have not been detected in vivo despite abundant defective HIV genomes (*22*, *65*), although the TIP deletion arrangement provides clues. Specifically, accumulation of DIP-like deletions requires $R_0 > 1$, but for HIV, this requires a complex series of multiple recombination-rearrangement events in which the cPPT-flanking sequences are deleted, but the cPPT itself is retained or reinserted (*65*).

From the translational perspective, future studies will be needed to evaluate the clinical potential of TIPs. For example, TIPs lacking GFP must be developed, though preliminary analyses indicate that such ΔGFP TIPs maintain equivalent efficacy (fig. S17B). Notably, TIPs will need to be tested in more realistic clinical intervention scenarios such as ATI studies (*90*) and assessed for genotoxicity, disease progression, and inflammatory signatures at later time points to determine whether TIP-treatment results in delayed disease HIV-1 long-term nonprogressors (*61*). It should be noted that TIPs are unlikely to be a sterilizing cure owing to their conditional replication requirement. However, as single-administration lentiviral vectors, TIPs can establish latency and reactivate upon HIV rebound (Fig. 5, A to C), thereby echoing calls for an HIV "functional cure."

Methods summary

Putative DIPs were identified from a continuous culture reactor where CEM $CD4^+$ cells were infected with replication-competent reporter virus (HIV-GFP or HIV-BFP) at multiplicity of infection (MOI) ~0.01 to 0.1 (virions/cell). Cells were followed over time through flow cytometry for GFP expression and cell viability to detect Von Magnus–like fluctuations. DNA was extracted from cells at day 71, and HIV DNA was amplified by PCR, leading to identification of the ~2.5-kb deletion. DIP VLPs were packaged on 293T cells and yield reduction, and transduction efficiency were assayed on MT4 cells.

TIP engineering was carried out, reintroducing the cPPT sequence into the DIP by restriction cloning to make TIP-1, and this construct was modified to ablate *tat*/*rev*/*vpu*/*env* expression resulting in TIP-2. Further optimization by introduction of two additional deletions (one in *gag*, the other in *env*) resulted in the optimized HIV-TIP construct (table S1). TIP transduction efficiencies were determined by titering packaged TIPs on MT4s in the presence of replication-competent HIV and normalizing titer units (TU) per ng of capsid protein.

For testing the efficacy of TIPs in $CD4^+$ primary cells, $CD4^+$ cells were purified from healthy donors activated with CD3/CD28 Dynabeads, then transduced with TIP and infected with HIV-BFP; cultures were supplemented with activated $CD4^+$ cells if required. Cells were monitored by flow cytometry for TIP-GFP and/or HIV-BFP expression over time. Similarly, TIP efficacy was tested in cell lines (CEMs, MT4s, and Jurkats), either through coinfection with TIP and HIV or pretransducing cells with TIP followed by HIV infection. Cultures were maintained by replacing media and assayed by flow cytometry. HIV and TIP proviral integration was assayed via qPCR using HIV and/or TIP specific primers (table S2).

R_0 quantification by three-color assay utilized stable polyclonal TIP-transduced cell lines with single TIP integrations created by transducing CEM cells with TIP at low MOI. The TIP stable cell lines ("producer" cells) were infected with HIV-BFP and after a single round of infection, cocultured with "target" cells, i.e., doxycycline-inducible Tat-mCherry cells, at a ratio of 1:20. After each single round infection, cells were subjected to flow cytometry to determine the percentage of BFP^+ cells in the "producer" cells and the BFP^+ and GFP^+ cells in the "target" cells. These values were then used to calculate R_0 values for TIP, as detailed in the materials and methods.

TIP in vivo efficacy was tested in two humanized mouse models: the PBMC NSG mouse model and the $CD34^+$ NSG model. For both model's mice were challenged with HIV at day 0 and treated with HIV-TIP lentiviral vector VLPs at day 5 through intravenous injection. Animals were bled weekly, and plasma viremia was assayed through qRT-PCR using HIV-1 specific primer-probes (table S2).

The SIV-TIP (table S1) was constructed from the SIVΔnef-eGFP molecular clone. Deletions were analogous to the optimized HIV-TIP and introduced using standard cloning methods. The SIV-TIP was pseudotyped with the SIV-specific envelope SIVmac251.6. Preliminary in vitro testing was carried out in rhesus macaque splenocytes transduced with SIV-TIP and then infected with SHIV SF162P3. At 7 days following infection, both cells and supernatant were collected, the cells were stained for p27 and CD45 and subjected to flow analysis. The supernatant was diluted and titered on TZM-bl cells by assaying for luciferase activity.

SIV-TIP efficacy was tested in infant rhesus macaques. 6 out of 10 animals were administered TIP 24 hours prior and all animals were then challenged with SHIV-SF162P3. Animals were bled weekly and followed until clinical end point. Plasma viremia and TIP levels were determined by RT-qPCR and digital droplet PCR (ddPCR), respectively, using SIV*gag* primers and GFP-specific primer probes (tables S2 and S3). PBMCs were isolated from plasma at day 0 (a day post TIP administration, preinfection), and DNA was extracted and subjected to qPCR to detect TIP-GFP DNA. Viral RNA was isolated from plasma, reverse transcribed and subjected to near full-length sequencing and phylogenetic analyses using Geneious software. Plasma viral loads were fit to the mathematical models of virus dynamics (as detailed in Supplementary text section 4)

Immune response (i.e., seroconversion) was assayed by enzyme-linked immunosorbent assay (ELISA) of plasma samples using recombinant HIV-1 SF162 gp140 trimer to determine binding titers. SHIV viral RNA quantification in end-point lymphoid tissues was determined by RNAScope as detailed in the materials and methods (see supplementary materials section "Seroconversion, immunohistochemistry, RNAscope in situ hybridization, and quantitative image analysis").

TIP efficacy in $CD4^+$ cells isolated from persons living with HIV [i.e., persons who inject drugs (PWID)] was tested similar to the above efficacy testing in $CD4^+$ primary cells. Patient CD4+ cells were isolated, activated and transduced with TIP, fresh activated $CD4^+$ cells from PWID and pre–TIP-transduced $CD4^+$ cells from healthy donors were added to propagate infection, culture supernatant was sampled over time and measured for p24 to assay HIV knockdown.

TIP latency, reversal, and associated reduction in HIV rebound was tested using a modified viral outgrowth assay: Jurkat cells were transduced with TIP, infected with HIV-BFP, and treated with Darunavir and Raltegravir until viral suppression was achieved. Cells were then washed to remove Darunavir and Raltegravir, diluted and cocultured with a fixed amount of MT4 target cells, and treated with tumor necrosis factor (TNF)–α to induce reactivation of latent HIV and TIP. Cultures were monitored daily, split as required, and analyzed by flow cytometry to measure the percentage of HIV-BFP and/or HIV-BFP TIP-GFP infected cells upon reactivation. To assay integration, cells were extracted at a given time point, the DNA was isolated, and then subjected to qPCR with HIV and/or TIP-specific primers (table S2).

For the $CD4^+$ depletion or protection assay, $CD4^+$ cells from healthy donors were isolated, activated, and TIP-transduced. A day later, cells were infected with HIV. Fresh primary T cell targets were added at day 7 to propagate the culture. Cells were extracted at days 3, 7, and 14 and analyzed by qPCR for TIP integration.

REFERENCES AND NOTES

1. Joint United Nations Programme on HIV/AIDS, "The path that ends AIDS: UNAIDS Global AIDS Update 2023" (UNAIDS, 2023).
2. R. T. Davey Jr. *et al*., HIV-1 and T cell dynamics after interruption of highly active antiretroviral therapy (HAART) in patients with a history of sustained viral suppression. *Proc. Natl. Acad. Sci. U.S.A.* **96**, 15109–15114 (1999). doi: 10.1073/pnas.96.26.15109; pmid: 10611346

3. M. C. Sneller *et al*., Kinetics of Plasma HIV Rebound in the Era of Modern Antiretroviral Therapy. *J. Infect. Dis.* **222**, 1655–1659 (2020). doi: 10.1093/infdis/jiaa270; pmid: 32443148
4. J. M. Coffin, HIV population dynamics in vivo: Implications for genetic variation, pathogenesis, and therapy. *Science* **267**, 483–489 (1995). doi: 10.1126/science.7824947; pmid: 7824947
5. R. M. Ribeiro, S. Bonhoeffer, Production of resistant HIV mutants during antiretroviral therapy. *Proc. Natl. Acad. Sci. U.S.A.* **97**, 7681–7686 (2000). doi: 10.1073/pnas.97.14.7681; pmid: 10884399
6. D. E. Goldberg, R. F. Siliciano, W. R. Jacobs Jr., Outwitting evolution: Fighting drug-resistant TB, malaria, and HIV. *Cell* **148**, 1271–1283 (2012). doi: 10.1016/j.cell.2012.02.021; pmid: 22424234
7. L. S. Weinberger, D. V. Schaffer, A. P. Arkin, Theoretical design of a gene therapy to prevent AIDS but not human immunodeficiency virus type 1 infection. *J. Virol.* **77**, 10028–10036 (2003). doi: 10.1128/JVI.77.18.10028-10036.2003; pmid: 12941913
8. V. T. Metzger, J. O. Lloyd-Smith, L. S. Weinberger, Autonomous targeting of infectious superspreaders using engineered transmissible therapies. *PLOS Comput. Biol.* **7**, e1002015 (2011). doi: 10.1371/journal.pcbi.1002015; pmid: 21483468
9. L. I. Rast *et al*., Conflicting Selection Pressures Will Constrain Viral Escape from Interfering Particles: Principles for Designing Resistance-Proof Antivirals. *PLOS Comput. Biol.* **12**, e1004799 (2016). doi: 10.1371/journal.pcbi.1004799; pmid: 27152856
10. I. M. Rouzine, L. S. Weinberger, Design requirements for interfering particles to maintain coadaptive stability with HIV-1. *J. Virol.* **87**, 2081–2093 (2013). doi: 10.1128/JVI.02741-12; pmid: 23221552
11. P. von Magnus, Incomplete forms of influenza virus. *Adv. Virus Res.* **2**, 59–79 (1954). doi: 10.1016/S0065-3527(08)60529-1; pmid: 13228257
12. R. Anderson, R. May, *Infectious Diseases of Humans* (Oxford Univ. Press, 1991). doi: 10.1093/oso/9780198545996.001.0001
13. S. Chaturvedi *et al*., Identification of a therapeutic interfering particle-A single-dose SARS-CoV-2 antiviral intervention with a high barrier to resistance. *Cell* **184**, 6022–6036.e18 (2021). doi: 10.1016/j.cell.2021.11.004; pmid: 34838159
14. S. Chaturvedi *et al*., A single-administration therapeutic interfering particle reduces SARS-CoV-2 viral shedding and pathogenesis in hamsters. *Proc. Natl. Acad. Sci. U.S.A.* **119**, e2204624119 (2022). doi: 10.1073/pnas.2204624119; pmid: 36074824
15. B. Dropulić, M. Hěrmánková, P. M. Pitha, A conditionally replicating HIV-1 vector interferes with wild-type HIV-1 replication and spread. *Proc. Natl. Acad. Sci. U.S.A.* **93**, 11103–11108 (1996). doi: 10.1073/pnas.93.20.11103; pmid: 8855316
16. B. L. Levine *et al*., Gene transfer in humans using a conditionally replicating lentiviral vector. *Proc. Natl. Acad. Sci. U.S.A.* **103**, 17372–17377 (2006). doi: 10.1073/pnas.0608138103; pmid: 17090675
17. D. S. An *et al*., An inducible human immunodeficiency virus type 1 (HIV-1) vector which effectively suppresses HIV-1 replication. *J. Virol.* **73**, 7671–7677 (1999). doi: 10.1128/JVI.73.9.7671-7677.1999; pmid: 10438857
18. E. Klimatcheva *et al*., Defective lentiviral vectors are efficiently trafficked by HIV-1 and inhibit its replication. *Mol. Ther.* **3**, 928–939 (2001). doi: 10.1006/mthe.2001.0344; pmid: 11407907
19. K. V. Morris, D. J. Looney, Characterization of human immunodeficiency virus (HIV)-2 vector mobilization by HIV-1. *Hum. Gene Ther.* **16**, 1463–1472 (2005). doi: 10.1089/hum.2005.16.1463; pmid: 16390277
20. X. Lu *et al*., Safe two-plasmid production for the first clinical lentivirus vector that achieves >99% transduction in primary cells using a one-step protocol. *J. Gene Med.* **6**, 963–973 (2004). doi: 10.1002/jgm.593; pmid: 15352069
21. W. Henle, G. Henle, Interference of Inactive Virus with the Propagation of Virus of Influenza. *Science* **98**, 87–89 (1943). doi: 10.1126/science.98.2534.87.b; pmid: 17749157
22. K. M. Bruner *et al*., Defective proviruses rapidly accumulate during acute HIV-1 infection. *Nat. Med.* **22**, 1043–1049 (2016). doi: 10.1038/nm.4156; pmid: 27500724
23. Y.-C. Ho *et al*., Replication-competent noninduced proviruses in the latent reservoir increase barrier to HIV-1 cure. *Cell* **155**, 540–551 (2013). doi: 10.1016/j.cell.2013.09.020; pmid: 24243014
24. A. S. Perelson, A. U. Neumann, M. Markowitz, J. M. Leonard, D. D. Ho, HIV-1 dynamics in vivo: Virion clearance rate, infected cell life-span, and viral generation time. *Science* **271**, 1582–1586 (1996). doi: 10.1126/science.271.5255.1582; pmid: 8599114
25. M. A. Nowak, R. M. May, *Virus dynamics: Mathematical principles of immunology and virology* (Oxford Univ. Press, 2000). doi: 10.1093/oso/9780198504184.001.0001
26. D. N. Levy, G. M. Aldrovandi, O. Kutsch, G. M. Shaw, Dynamics of HIV-1 recombination in its natural target cells. *Proc. Natl. Acad. Sci. U.S.A.* **101**, 4204–4209 (2004). doi: 10.1073/pnas.0306764101; pmid: 15010526
27. P. von Magnus, Propagation of the PR8 strain of influenza A virus in chick embryos. II. The formation of incomplete virus following inoculation of large doses of seed virus. *Acta Pathol. Microbiol. Scand.* **28**, 278–293 (1951). doi: 10.1111/j.1699-0463.1951.tb03693.x; pmid: 14856732
28. P. Charneau, M. Alizon, F. Clavel, A second origin of DNA plus-strand synthesis is required for optimal human immunodeficiency virus replication. *J. Virol.* **66**, 2814–2820 (1992). doi: 10.1128/jvi.66.5.2814-2820.1992; pmid: 1560526
29. V. Dardalhon *et al*., Lentivirus-mediated gene transfer in primary T cells is enhanced by a central DNA flap. *Gene Ther.* **8**, 190–198 (2001). doi: 10.1038/sj.gt.3301378; pmid: 11313790
30. A. Follenzi, L. E. Ailles, S. Bakovic, M. Geuna, L. Naldini, Gene transfer by lentiviral vectors is limited by nuclear translocation and rescued by HIV-1 pol sequences. *Nat. Genet.* **25**, 217–222 (2000). doi: 10.1038/76095; pmid: 10835641
31. F. Park, M. A. Kay, Modified HIV-1 based lentiviral vectors have an effect on viral transduction efficiency and gene expression in vitro and in vivo. *Mol. Ther.* **4**, 164–173 (2001). doi: 10.1006/mthe.2001.0450; pmid: 11545606
32. B. Van Maele, J. De Rijck, E. De Clercq, Z. Debyser, Impact of the central polypurine tract on the kinetics of human immunodeficiency virus type 1 vector transduction. *J. Virol.* **77**, 4685–4694 (2003). doi: 10.1128/JVI.77.8.4685-4694.2003; pmid: 12663775
33. T. Notton, J. J. Glazier, V. R. Saykally, C. E. Thompson, L. S. Weinberger, RanDeL-Seq: A High-Throughput Method to Map Viral *cis*- and *trans*-Acting Elements. *mBio* **12**, e01724-20 (2021). doi: 10.1128/mBio.01724-20; pmid: 33468683
34. M. A. Nowak *et al*., Viral dynamics of primary viremia and antiretroviral therapy in simian immunodeficiency virus infection. *J. Virol.* **71**, 7518–7525 (1997). doi: 10.1128/jvi.71.10.7518-7525.1997; pmid: 9311831
35. C. L. Althaus, A. S. De Vos, R. J. De Boer, Reassessing the human immunodeficiency virus type 1 life cycle through age-structured modeling: Life span of infected cells, viral generation time, and basic reproductive number, R0. *J. Virol.* **83**, 7659–7667 (2009). doi: 10.1128/JVI.01799-08; pmid: 19457999
36. A. Lever, H. Gottlinger, W. Haseltine, J. Sodroski, Identification of a sequence required for efficient packaging of human immunodeficiency virus type 1 RNA into virions. *J. Virol.* **63**, 4085–4087 (1989). doi: 10.1128/jvi.63.9.4085-4087.1989; pmid: 2760989
37. M. Kuzembayeva, K. Dilley, L. Sardo, W. S. Hu, Life of psi: How full-length HIV-1 RNAs become packaged genomes in the viral particles. *Virology* **454-455**, 362–370 (2014). doi: 10.1016/j.virol.2014.01.019; pmid: 24530126
38. M. D. Marsden, J. A. Zack, Humanized Mouse Models for Human Immunodeficiency Virus Infection. *Annu. Rev. Virol.* **4**, 393–412 (2017). doi: 10.1146/annurev-virology-101416-041703; pmid: 28746819
39. L. Holguin, L. Echavarria, J. C. Burnett, Novel Humanized Peripheral Blood Mononuclear Cell Mouse Model with Delayed Onset of Graft-versus-Host Disease for Preclinical HIV Research. *J. Virol.* **96**, e0139421 (2022). doi: 10.1128/JVI.01394-21; pmid: 34818071
40. R. S. Leibman *et al*., Supraphysiologic control over HIV-1 replication mediated by CD8 T cells expressing a re-engineered CD4-based chimeric antigen receptor. *PLOS Pathog.* **13**, e1006613 (2017). doi: 10.1371/journal.ppat.1006613; pmid: 29023549
41. R. Mukherjee *et al*., HIV sequence variation associated with env antisense adoptive T-cell therapy in the hNSG mouse model. *Mol. Ther.* **18**, 803–811 (2010). doi: 10.1038/mt.2009.316; pmid: 20104212
42. D. H. Barouch *et al*., Therapeutic efficacy of potent neutralizing HIV-1-specific monoclonal antibodies in SHIV-infected rhesus monkeys. *Nature* **503**, 224–228 (2013). doi: 10.1038/nature12744; pmid: 24172905
43. M. Shingai *et al*., Antibody-mediated immunotherapy of macaques chronically infected with SHIV suppresses viraemia. *Nature* **503**, 277–280 (2013). doi: 10.1038/nature12746; pmid: 24172896
44. A. J. Hessell, N. L. Haigwood, Animal models in HIV-1 protection and therapy. *Curr. Opin. HIV AIDS* **10**, 170–176 (2015). doi: 10.1097/COH.0000000000000152; pmid: 25730345
45. A. J. Hessell *et al*., Early short-term treatment with neutralizing human monoclonal antibodies halts SHIV infection in infant macaques. *Nat. Med.* **22**, 362–368 (2016). doi: 10.1038/nm.4063; pmid: 26998834
46. M. B. Shapiro *et al*., Single-dose bNAb cocktail or abbreviated ART post-exposure regimens achieve tight SHIV control without adaptive immunity. *Nat. Commun.* **11**, 70 (2020). doi: 10.1038/s41467-019-13972-y; pmid: 31911610
47. P. A. Luciw, E. Pratt-Lowe, K. E. Shaw, J. A. Levy, C. Cheng-Mayer, Persistent infection of rhesus macaques with T-cell-line-tropic and macrophage-tropic clones of simian/human immunodeficiency viruses (SHIV). *Proc. Natl. Acad. Sci. U.S.A.* **92**, 7490–7494 (1995). doi: 10.1073/pnas.92.16.7490; pmid: 7638218
48. A. N. Nelson *et al*., Simian-Human Immunodeficiency Virus SHIV.CH505-Infected Infant and Adult Rhesus Macaques Exhibit Similar Env-Specific Antibody Kinetics, despite Distinct T-Follicular Helper and Germinal Center B Cell Landscapes. *J. Virol.* **93**, e00168-19 (2019). doi: 10.1128/JVI.00168-19; pmid: 31092583
49. R. Goswami *et al*., Analytical treatment interruption after short-term antiretroviral therapy in a postnatally simian-human immunodeficiency virus-infected infant rhesus macaque model. *mBio* **10**, e01971-19 (2019). doi: 10.1128/mBio.01971-19; pmid: 31488511
50. P. A. Luciw *et al*., Fatal immunopathogenesis by SIV/HIV-1 (SHIV) containing a variant form of the HIV-1SF33 env gene in juvenile and newborn rhesus macaques. *Virology* **263**, 112–127 (1999). doi: 10.1006/viro.1999.9908; pmid: 10544087
51. L. Micci *et al*., CD4 depletion in SIV-infected macaques results in macrophage and microglia infection with rapid turnover of infected cells. *PLOS Pathog.* **10**, e1004467 (2014). doi: 10.1371/journal.ppat.1004467; pmid: 25356757
52. K. K. Van Rompay *et al*., Immunization of newborn rhesus macaques with simian immunodeficiency virus (SIV) vaccines prolongs survival after oral challenge with virulent SIVmac251. *J. Virol.* **77**, 179–190 (2003). doi: 10.1128/JVI.77.1.179-190.2003; pmid: 12477823
53. D. J. Hartigan-O'Connor, K. Abel, J. M. McCune, Suppression of SIV-specific CD4+ T cells by infant but not adult macaque regulatory T cells: Implications for SIV disease progression. *J. Exp. Med.* **204**, 2679–2692 (2007). doi: 10.1084/jem.20071068; pmid: 17954571
54. R. A. Reyes *et al*., Induction of simian AIDS in infant rhesus macaques infected with CCR5- or CXCR4-utilizing simian-human immunodeficiency viruses is associated with distinct lesions of the thymus. *J. Virol.* **78**, 2121–2130 (2004). doi: 10.1128/JVI.78.4.2121-2130.2004; pmid: 14747577
55. C. Deleage *et al*., Defining HIV and SIV reservoirs in lymphoid tissues. *Pathog. Immun.* **1**, 68–106 (2016). doi: 10.20411/pai.v1i1.100; pmid: 27430032
56. F. Wang *et al*., RNAscope: A novel in situ RNA analysis platform for formalin-fixed, paraffin-embedded tissues. *J. Mol. Diagn.* **14**, 22–29 (2012). doi: 10.1016/j.jmoldx.2011.08.002; pmid: 22166544
57. A. S. Perelson, Modelling viral and immune system dynamics. *Nat. Rev. Immunol.* **2**, 28–36 (2002). doi: 10.1038/nri700; pmid: 11905835
58. D. B. Reeves, C. W. Peterson, H. P. Kiem, J. T. Schiffer, Autologous Stem Cell Transplantation Disrupts Adaptive Immune Responses during Rebound Simian/Human Immunodeficiency Virus Viremia. *J. Virol.* **91**, e00095-17 (2017). doi: 10.1128/JVI.00095-17; pmid: 28404854
59. J. Schröter, R. J. de Boer, What explains the poor contraction of the viral load during paediatric HIV infection? *J. Theor. Biol.* **570**, 111521 (2023). doi: 10.1016/j.jtbi.2023.111521; pmid: 37164225
60. A. Durudas *et al*., Elevated levels of innate immune modulators in lymph nodes and blood are associated with more-rapid disease progression in simian immunodeficiency virus-infected monkeys. *J. Virol.* **83**, 12229–12240 (2009). doi: 10.1128/JVI.01311-09; pmid: 19759147
61. L. Capa *et al*., Elite controllers long-term non progressors present improved survival and slower disease progression. *Sci. Rep.* **12**, 16356 (2022). doi: 10.1038/s41598-022-19970-3; pmid: 36175445

62. L. S. Weinberger, J. C. Burnett, J. E. Toettcher, A. P. Arkin, D. V. Schaffer, Stochastic gene expression in a lentiviral positive-feedback loop: HIV-1 Tat fluctuations drive phenotypic diversity. *Cell* **122**, 169–182 (2005). doi: 10.1016/j.cell.2005.06.006; pmid: 16051143
63. B. S. Razooky, A. Pai, K. Aull, I. M. Rouzine, L. S. Weinberger, A hardwired HIV latency program. *Cell* **160**, 990–1001 (2015). doi: 10.1016/j.cell.2015.02.009; pmid: 25723172
64. M. M. K. Hansen *et al*., A Post-Transcriptional Feedback Mechanism for Noise Suppression and Fate Stabilization. *Cell* **173**, 1609–1621. e15 (2018). doi: 10.1016/j.cell.2018.04.005; pmid: 29754821
65. K. M. Bruner *et al*., A quantitative approach for measuring the reservoir of latent HIV-1 proviruses. *Nature* **566**, 120–125 (2019). doi: 10.1038/s41586-019-0898-8; pmid: 30700913
66. J. J. Rose *et al*., CD4 down-regulation by HIV-1 and simian immunodeficiency virus (SIV) Nef proteins involves both internalization and intracellular retention mechanisms. *J. Biol. Chem.* **280**, 7413–7426 (2005). doi: 10.1074/jbc.M409420200; pmid: 15611114
67. C. A. Lundquist, M. Tobiume, J. Zhou, D. Unutmaz, C. Aiken, Nef-mediated downregulation of CD4 enhances human immunodeficiency virus type 1 replication in primary T lymphocytes. *J. Virol.* **76**, 4625–4633 (2002). doi: 10.1128/JVI.76.9.4625-4633.2002; pmid: 11932428
68. C. R. Maldini *et al*., HIV-Resistant and HIV-Specific CAR-Modified $CD4^+$ T Cells Mitigate HIV Disease Progression and Confer $CD4^+$ T Cell Help In Vivo. *Mol. Ther.* **28**, 1585–1599 (2020). doi: 10.1016/j.ymthe.2020.05.012; pmid: 32454027
69. N. L. Galloway *et al*., Cell-to-cell transmission of HIV-1 is required to trigger pyroptotic death of lymphoid-tissue-derived CD4 T cells. *Cell Rep.* **12**, 1555–1563 (2015). doi: 10.1016/j.celrep.2015.08.011; pmid: 26321639
70. G. Doitsh *et al*., Cell death by pyroptosis drives CD4 T-cell depletion in HIV-1 infection. *Nature* **505**, 509–514 (2014). doi: 10.1038/nature12940; pmid: 24356306
71. P. W. Denton *et al*., Targeted cytotoxic therapy kills persisting HIV infected cells during ART. *PLOS Pathog.* **10**, e1003872 (2014). doi: 10.1371/journal.ppat.1003872; pmid: 24415939
72. Z. Sun *et al*., Intrarectal transmission, systemic infection, and CD4+ T cell depletion in humanized mice infected with HIV-1. *J. Exp. Med.* **204**, 705–714 (2007). doi: 10.1084/jem.20062411; pmid: 17389241
73. C. Fraser, T. D. Hollingsworth, R. Chapman, F. de Wolf, W. P. Hanage, Variation in HIV-1 set-point viral load: Epidemiological analysis and an evolutionary hypothesis. *Proc. Natl. Acad. Sci. U.S.A.* **104**, 17441–17446 (2007). doi: 10.1073/pnas.0708559104; pmid: 17954909
74. W. H. Organization, *Consolidated guidelines on HIV prevention, testing, treatment, service delivery and monitoring: Recommendations for a public health approach* (World Health Organization, 2021).
75. A. S. Perelson, P. Essunger, D. D. Ho, Dynamics of HIV-1 and CD4+ lymphocytes in vivo. *AIDS* **11** (Suppl A), S17–S24 (1997). pmid: 9451962
76. R. Batorsky *et al*., Estimate of effective recombination rate and average selection coefficient for HIV in chronic infection. *Proc. Natl. Acad. Sci. U.S.A.* **108**, 5661–5666 (2011). doi: 10.1073/pnas.1102036108; pmid: 21436045
77. D. P. Wooley, R. A. Smith, S. Czajak, R. C. Desrosiers, Direct demonstration of retroviral recombination in a rhesus monkey. *J. Virol.* **71**, 9650–9653 (1997). doi: 10.1128/jvi.71.12.9650-9653.1997; pmid: 9371629
78. L. Josefsson *et al*., Majority of CD4+ T cells from peripheral blood of HIV-1-infected individuals contain only one HIV DNA molecule. *Proc. Natl. Acad. Sci. U.S.A.* **108**, 11199–11204 (2011). doi: 10.1073/pnas.1107729108; pmid: 21690402
79. P. Tebas *et al*., Antiviral effects of autologous CD4 T cells genetically modified with a conditionally replicating lentiviral vector expressing long antisense to HIV. *Blood* **121**, 1524–1533 (2013). doi: 10.1182/blood-2012-07-447250; pmid: 23264589
80. M. C. Milone, U. O'Doherty, Clinical use of lentiviral vectors. *Leukemia* **32**, 1529–1541 (2018). doi: 10.1038/s41375-018-0106-0; pmid: 29654266
81. G. J. McGarrity *et al*., Patient monitoring and follow-up in lentiviral clinical trials. *J. Gene Med.* **15**, 78–82 (2013). doi: 10.1002/jgm.2691; pmid: 23322669
82. H. Katano *et al*., Integration of HIV-1 caused STAT3-associated B cell lymphoma in an AIDS patient. *Microbes Infect.* **9**, 1581–1589 (2007). doi: 10.1016/j.micinf.2007.09.008; pmid: 18024124
83. N. Verdun, P. Marks, Secondary cancers after chimeric antigen receptor T-cell therapy. *N. Engl. J. Med.* **390**, 584–586 (2024). doi: 10.1056/NEJMp2400209; pmid: 38265704
84. M. W. Parsons *et al*., Secondary malignancies in non-Hodgkin lymphoma survivors: 40 years of follow-up assessed by treatment modality. *Cancer Med.* **12**, 2624–2636 (2023). doi: 10.1002/cam4.5139; pmid: 36812123
85. B. Shbib Dabaja *et al*., Second malignancies in patients with Hodgkin's Lymphoma: Half a century of experience. *Clin. Transl. Radiat. Oncol.* **35**, 64–69 (2022). doi: 10.1016/j.ctro.2022.04.011; pmid: 35601797
86. Y. Yu *et al*., Second malignant neoplasms in lymphomas, secondary lymphomas and lymphomas in metabolic disorders/diseases. *Cell Biosci.* **12**, 30 (2022). doi: 10.1186/s13578-022-00763-0; pmid: 35279210
87. J. W. Mellors *et al*., Insertional activation of *STAT3* and *LCK* by HIV-1 proviruses in T cell lymphomas. *Sci. Adv.* **7**, eabi8795 (2021). doi: 10.1126/sciadv.abi8795; pmid: 34644108
88. J. K. Yoon *et al*., HIV proviral DNA integration can drive T cell growth ex vivo. *Proc. Natl. Acad. Sci. U.S.A.* **117**, 32880–32882 (2020). doi: 10.1073/pnas.2013194117; pmid: 33318172
89. T. Notton, J. Sardanyés, A. D. Weinberger, L. S. Weinberger, The case for transmissible antivirals to control population-wide infectious disease. *Trends Biotechnol.* **32**, 400–405 (2014). doi: 10.1016/j.tibtech.2014.06.006; pmid: 25017994
90. B. Julg *et al*., Recommendations for analytical antiretroviral treatment interruptions in HIV research trials-report of a consensus meeting. *Lancet HIV* **6**, e259–e268 (2019). doi: 10.1016/S2352-3018(19)30052-9; pmid: 30885693
91. F. Pitchai, N. Khetan, Code and data for: Engineered deletions of HIV replicate conditionally to reduce disease in non-human primates, Zenodo (2024); https://zenodo.org/doi/10.5281/zenodo.10970896.

ACKNOWLEDGMENTS

We thank C. Mello, D. Richman, K. Jerome, and the Weinberger Lab for discussions and suggestions. We thank M. Wolf for extensive technical support and C. Ignacio for isolating human PBMCs. We are grateful to R. Basavappa for enabling pilot exploration of the TIP concept, J. Gimlett for initiating the DARPA INTERCEPT program for TIP engineering, and W. Sammons-Jackson and D. Bacon for championing safety and efficacy testing of TIPs. We thank K. Claiborn for editing and the Gladstone-UCSF CFAR flow cytometry core, supported by NIH P30 AI027763, S10 RR028962, and the James B. Pendleton Charitable Trust for technical support. The following reagents were obtained through the NIH AIDS Reagent Program, Division of AIDS, NIAID, NIH: MT-4 cells from D. Richman and CEM CD4+ cells from J. P. Jacobs (cat. # 117). We also thank H. Watry and B. Conklin from Gladstone Institutes and E. Chow from the UCSF Center for Advanced Technology (CAT) for access to ddPCR equipment and advice in developing the ddPCR assay. We thank X. Chen for manuscript review and feedback. **Funding:** This work was supported by the DARPA INTERCEPT program (D17AC00009), the NIH Director's New Innovator (OD006677) and Pioneer Award (OD17181 and DA051144) programs, an NIH MERIT award (R37AI109593), and the US Army Medical Infectious Disease Research Program (MT19010.08). Animals at Oregon National Primate Research Center were funded by MT19010.08, P51-OD011092, and U42-OD010426. This project was funded in part with federal funds from the National Cancer Institute, National Institutes of Health, under contract nos. 75N91019D00024/HHSN261201500003I and R01DA049644. The content of this publication does not necessarily reflect the views or policies of the Department of Health and Human Services, nor does the mention of trade names, commercial products, or organizations imply endorsement by the US government. **Author contributions:** L.S.W. conceived and designed the studies. N.L.H. and L.S.W. designed the rhesus macaque studies. F.N.N.P., E.J.T., N.K., G.V., C.L., A.J.K., S.P., T.O., P.B., D.S., S.-Y.J, J.G., C.T., A.H.-V., H.-I.S., L.H., R.U., W.B., K.B.-S., J.B., J.D.E., A.H., B.F.K., and C.M.F. designed and performed the experiments and curated the data. A.H.-V. and S.A.S. provided HIV^+ participant samples. L.S.W. wrote the paper. **Competing interests:** L.S.W. is an equity cofounder of VxBiosciences Inc and Autonomous Therapeutics Inc. L.S.W., E.J.T., and S.-Y.J. are inventors on patent or patent application US17/619,063 held by the J. David Gladstone Institutes that covers composition and methods for HIV-1 TIPs. The other authors declare that they have no competing interests. **Data and materials availability:** The data that support the findings of this study are available from the corresponding author upon request. All biological materials are available from the corresponding author. Sequencing data has been deposited in GenBank (accession nos. PP597405 to PP597522 and PP646066 to PP646153). Custom code for mathematical modeling is available on GitHub at https://github.com/khetanneha/HIV-SIV-TIP-Modeling and archived on Zenodo along with all the experimental raw data (*91*). An MTA for the HIV Reagent program is available on request from the corresponding author under an agreement with J. David Gladstone Institutes.

SUPPLEMENTARY MATERIALS

science.org/doi/10.1126/science.adn5866
Material and Methods
Supplementary Text
Figs. S1 to S17
Tables S1 to S3
References (*92*–*119*)
Data S1

Submitted 17 December 2023; accepted 6 June 2024
10.1126/science.adn5866